ARTICLE
Traditional Medicine Research 2024;9(5):29. https://doi.org/10.53388/TMR20231115003

Metabolic profiling and anti-inflammatory verification in the ethnic herbal medicine Trachelospermi Caulis et Folium

Zi-Hong Huang[1], Chun-Hua Lai[2], Bang-Yong Wang[1], Bin-Sheng Luo[3], Edward James Kennelly[4*], Qin-Gang Tan[1, 4, 5*]

[1]Department of Medicinal Chemistry, School of Pharmaceutical Sciences, Guilin Medical University, Guilin 541199, China. [2]Department of Traditional Chinese Medicine, Affiliated Hospital of Guilin Medical University, Guilin 541001, China. [3]Lushan Botanical Garden, Jiangxi Province and Chinese Academy of Sciences, Lushan 332900, China. [4]Department of Biological Sciences, Lehman College, City University of New York, Bronx, New York 10468, USA. [5]State Key Laboratory of Phytochemistry and Plant Resources in West China, Kunming Institute of Botany, Chinese Academy of Sciences, Kunming 650201, China.

[*]**Correspondence to:** Edward J Kennelly, Department of Biological Sciences, Lehman College, City University of New York, 250 Bedford Park Boulevard West, New York 10468, USA. E-mail: edward.kennelly@lehman.cuny.edu. Qin-Gang Tan, Department of Medicinal Chemistry, School of Pharmaceutical Sciences, Guilin Medical University, 1 Zhiyuan Road, Guilin 541199, China. E-mail: qgtan@glmc.edu.cn.

Abstract

Background: Trachelospermi Caulis et Folium, the stems and leaves of *Trachelospermum jasminoides* (Lindl.) Lem, has been used as a remedy for rheumatism, gonarthritis, backache and pharyngitis, according to the *Chinese Pharmacopoeia*. However, the corresponding chemical substances of this ethnic medicinal plant with anti-inflammatory activity kept unclear. This study aimed to explore the active substances attribute to its anti-rheumatic activity of this medical plant. **Methods:** Ultra-high performance liquid chromatography combined with quadrupole time-of-flight mass spectrometry was used to identify the chemical components in the extract of *T. jasminoides*. Molecular docking was applied to analyze the binding affinity of potential active lignans to inducible nitric oxide synthase enzyme. The anti-inflammatory effects of the potential active fraction were verified by cell experiments in vitro. **Results:** Forty-one compounds, mainly are lignans and nine of which were reported for the first time from the genus of *Trachelospermum*, were characterized using ultra-high performance liquid chromatography quadrupole-time-of-flight mass spectrometry method. Molecular docking results showed these identified lignans had excellent interactions with the inducible nitric oxide synthase enzyme, and the lignans-enriched fraction could significantly inhibit the release of nitric oxide and the expression of inducible nitric oxide synthase protein in LPS-induced RAW264.7 cells. **Conclusion:** Lignans are the main active substances that responsible for the anti-inflammatory activity of the ethnic herbal medicine *T. jasminoides*.

Keywords: Trachelospermi Caulis et Folium; UPLC-QTOF-MS; molecular docking; NO inhibitory effect; lignans

Author contributions

Huang ZH performed the experiments, analyzed the data, and wrote the article. Lai CH collected the samples. Wang BY practiced the molecular docking. Kennelly EJ and Luo BS supervised this project and revised the article. Tan QG designed the experiments and provided funding for the research.

Competing interests

The authors declare no conflicts of interest.

Acknowledgments

This research was funded by National Natural Science Foundation of China (82060783) and the Fund of State Key Laboratory of Phytochemistry and Plant Resources in West China, Chinese Academy of Sciences (P2022-KF13).

Peer review information

Traditional Medicine Research thanks all anonymous reviewers for their contribution to the peer review of this paper.

Abbreviations

UPLC-QTOF-MS, ultra-high performance liquid chromatography quadrupole-time-of-flight mass spectrometry; iNOS, inducible nitric oxide synthase; NO, nitric oxide; LPS, lipopolysaccharides; PDB, Protein Data Bank.

Citation

Huang ZH, Lai CH, Wang BY, Luo BS, Kennelly EJ, Tan QG. Metabolic profiling and anti-inflammatory verification in the ethnic herbal medicine Trachelospermi Caulis et Folium. *Tradit Med Res*. 2024;9(5):29. doi: 10.53388/TMR20231115003.

Executive editor: Jing-Yi Wang.

Received: 15 November 2023; **Accepted:** 31 December 2023; **Available online:** 04 January 2024.

Highlights

Forty-one compounds were tentatively identified from Trachelospermi Caulis et Folium, in which nine compounds were reported for the first time in genus *Trachelospermum*. Lignans had excellent interactions with inducible nitric oxide synthase enzyme using molecular docking method. Lignans are the chemical substance of Trachelospermi Caulis et Folium for the treatment of inflammation-related disease.

Medical history of objective

Trachelospermi Caulis et Folium, has long been used a phototherapy on rheumatism, gonarthritis, backache and pharyngitis. It was recorded in *Compendium of Materia Medica* written by Shi-Zhen Li (1552–1578 C.E.) and other ethnic medical treatise such as *Shui Medicine, She Medicine*, and *Dong Medicine*. Modern research showed that the constituents such as lignans, flavonoids, triterpenoids, and alkaloids of this medicinal plant exhibited antioxidant, anti-inflammatory, anti-fatigue and cytotoxic effects.

Background

Trachelospermum jasminoides (Lindl.) Lem., a liana from the Apocynaceae family native to China, Japan, Korean and Vietnam, is widely recognized as luoshiteng in China. Trachelospermi Caulis et Folium, the dried stems and leaves of this plant, are extensively utilized as a phytotherapy resource, as documented in the *Chinese Pharmacopoeia* and ethnic pharmaceutical treatise [1, 2]. *T. jasminoides*, revered as an ethnic herbal medicine among the Shui, Dong, She, and Miao communities, has been demonstrated to alleviate various inflammation-related ailments, including rheumatoid arthritis, skin infections, and chronic bronchitis [3]. Compounds isolated from the genus *Trachelospermum* primarily include lignans, flavonoids, and triterpenes, exhibiting anti-inflammatory, analgesic, antitumor, antiviral, and antibacterial properties [1, 4]. Inflammation, a multifaceted process, undermines the immune system by activating various immune cells [5]. During the initial phase of inflammation, mediators such as NO, a signaling molecule generated by various cells within the body and be catalyzed by a group of enzymes known as nitric oxide synthases (NOS) including the inducible nitric oxide synthase (iNOS), play a pivotal role in orchestrating the inflammatory response [6]. Identification of iNOS inhibitors is a promising approach to prevent acute and chronic inflammatory states [7, 8]. Elevated concentrations of NO or persistent inflammation status lead to cellular damage and chronic inflammatory diseases, such as cardiovascular diseases and rheumatoid arthritis [9]. This mechanism is instrumental in escalating inflammation and is implicated in myriad biological processes [10, 11].

Traditional separation methods are often time-consuming, labor-intensive and requiring a significant amount of medicinal materials. In contrast, UPLC-QTOF-MS is widely acknowledged for its speed, accuracy, and reliability, making it a preferred choice for analytical tasks. This method has been extensively employed to bolster the analysis of Traditional Chinese Medicine as documented in the *Chinese Pharmacopoeia* [12–14]. Chinese medicinal materials have been a prolific source of compounds, contributing to developing novel immunotherapies for treating human disease [15]. UPLC-QTOF-MS technology was utilized to profile the typical metabolites in *T. jasminoide*, and a molecular docking study was subsequently conducted to assess the interactions of these characterized components with the iNOS enzyme. The Griess method was applied in vitro to validate the NO inhibitory efficacy of the fraction which containing the constituents of those showed a stronger binding affinity with iNOS derived from this plant. Collectively, these approaches provide novel insight into the anti-inflammatory activity of the active fraction obtained from this medicinal plant.

Material and methods

Plant collection

The stems and leaves of *T. jasminoides* were collected in March 2021 from Guilin, China. The plant material was authenticated by Professor Deqing Huang of Guilin Medical University. A voucher specimen (T-tj202103) has been deposited in the Experimental Centre of the School of Pharmaceutical Science at Guilin Medical University.

Reagents and materials

MS grade acetonitrile, methanol, water, and formic acid were sourced from Honeywell International Company (Maurice, NJ, USA). The AcroPrep™ Advance 0.45 μm PTFE filter was obtained from Pall Corporation (New York, NY, USA).

The UPLC-QTOF-MS system, comprising the Acquity UPLC liquid chromatograph and the Xevo G2-S Q-TOF mass spectrometer equipped with a Lockspray interface and electrospray ion source, was secured from Waters Corporation (Milford, MA, USA). Data collection and processing were facilitated through the MassLynx 4.1 mass spectrometry workstation. The Acquity UPLC BEH C_{18} column (2.1 mm × 100 mm, 1.7 μm) was also procured from Waters Corporation (Milford, MA, USA). The S30h-d78224 ultrasonic cleaner was acquired from Elma Schmidbauer GmbH (Hohentwiel, Germany). The analytical balance AL204 was sourced from Mettler-Toledo International Inc. (Zurich, Switzerland). The Model 3111 CO_2 incubator was obtained from Thermo Fisher Scientific Co., Ltd. (Waltham, MA, USA). High glucose Dulbecco's modified Eagle's medium (C11995500BT), Fetal bovine serum (10099141C), and 0.25% trypsin-EDTA were procured from Gibco Brl (BL512B, Grand Island, NY, USA). 3-(4,5-Dimethyl thiazole-2)-2,5-diphenyltetrazolium bromide salt (MTT, IM0280) and dimethyl sulfoxide (DMSO, D8371) for cell viability assay were obtained from Beijing Solarbio Science & Technology Co., Ltd. (Beijing, China). Indomethacin (53-86-1) and lipopolysaccharide (L2630) were sourced from Sigma-Aldrich Co., Ltd. (St. Louis, MO, USA), whereas the nitric oxide assay kit (S0021S) was purchased from Shanghai Beyotime Biological Co., Ltd. (Shanghai, China). Monoclonal antibodies against iNOS (E1A8233B-3, 1:1,000), β-actin (E12-041-3, 1:1,000), and peroxidase-conjugated secondary antibody (SA00001-2, 1:5,000) were procured from Cell Signaling Technology (Danvers, MA, USA). The Ac2-4s1 Biosafety Cabinet was acquired from Esco Micro Pte. Ltd. (Singapore) and the Infinite M200 PRO Multifunctional microplate reader was sourced from TECAN Group Company (Männedorf, Switzerland). The electrophoresis system, transmembrane system, and chemiluminescence imaging system were provided by Bio-Rad Corporation (Hercules, CA, USA).

Preparation of samples for UPLC-QTOF-MS analysis

Each dried stems and leaves of *T. jasminoides,* weighing 0.2 grams, was subjected to ultrasonic extraction twice at room temperature. During each extraction, 20 mL of a 4:1 (v/v) methanol-water mixture was employed, with each extraction lasting 20 min. The resultant supernatants were filtered using a 0.45 μm PTFE filter. The filtrates were prepared as samples at a concentration of 2 mg/mL. Prior to analysis, equal volumes of each extract were amalgamated to prepare the quality control (QC) sample. Subsequently, the pooled sample was dried under a nitrogen flow and stored at −20 °C.

Component analysis

For elution, the Acquity UPLC BEH C_{18} column (2.1 mm × 100 mm, 1.7 μm) was utilized at a flow rate of 0.5 mL/min. The mobile phase comprised a mixture of 0.1% formic acid in an aqueous solution (A) and acetonitrile (B). The elution procedure was sequenced as follows: 0–1.00 min, 5%–18% B; 1.00–2.50 min, 18%–20% B; 2.50–4.50 min, 20%–25% B; 4.50–5.00 min, 25%–70% B; 5.00–7.00 min, 70%–75% B; 7.00–9.50 min, 75%–98% B; 9.50–11.50 min, 98%–5% B; 11.50–13.50 min, 5% B.

Electrospray ionization in the negative polarity mode was employed with settings as follows: sample probe capillary voltage of 2.42 kV,

sampling cone voltage of 25 V, extraction cone voltage of 4 V, source temperature of 120 ˚C, and desolvation temperature of 550 ˚C. Nitrogen gas served as both the desolvation and cone gas, with flow rates set at 800 L/h and 20 L/h, respectively. Data were captured in the centroid mode using MS^E, with a low collision energy of 6 eV and a high collision energy ramp ranging from 20 V to 50 V. Data acquisition spanned a mass range of 100 to 1,500 Da and a retention time range of 0 to 13.5 min, with a scan time of 0.2 seconds. Data acquisition and processing were facilitated through the MassLynx 4.1 mass spectrometry workstation. The precise molecular mass and fragment information of the compounds were ascertained using the MassLynx 4.1 chromatographic workstation in conjunction with Progenesis QI software. Linamarin was employed as the inner standard, and pertinent literature was consulted [1, 16–25].

Molecular docking study

Chemical structures were initially delineated using ChemDraw program and subsequently converted to their three-dimensional (3D) coordinates using Chem3D. Each structure underwent energy minimization via the MM2 method and was saved in “pdb” format. The iNOS *Homo sapiens* protein code P35228 was sourced from the UniProt website (www.uniprot.org), and its X-ray crystal structure, with a resolution of 2.20 Å, was obtained from the Protein Data Bank (PDB) at the Research Collaboration for Structural Bioinformatics (https://www.rcsb.org) (PDB ID: 3E7G) [26]. Binding sites were identified using the site finder tool in Molecular Operating Environment 2019.0102, using the co-crystallized AR-C95791 as a reference. In the docking simulations, receptors were treated as rigid, and ligands as flexible. The “Triangle Matcher” method, coupled with an induced fit refinement model, was employed for the docking analysis. Here, each conformation per ligand was scored using the “London dG” scoring function, followed by a refinement step based on molecular mechanics and re-scoring with the “GBVI/WSA dG” scoring function [27, 28]. The docking process generated 50 poses per compound, from which five confirmations for each compound were selected for further analysis. Indomethacin served as a reference compound, having been experimentally proven to inhibit iNOS to a certain extent [29].

Preparation of lignans-enriched fraction

The methanol-water (1:4) extract solution of *T. jasminoide* was concentrated, dissolved in water, and loaded onto an AB-8 macroporous resin column, eluting with ethanol at concentrations ranging from 10% to 100%. The obtained 45% and 75% ethanol fractions, primarily composed of lignans, were preliminary considered as potential active fractions [30, 31]. The combined lignans-enriched fraction was dissolved using cell-grade DMSO, filtered through a sterile filter, and stored at 4 ˚C in a refrigerator. Prior to in vitro experiments, the samples were diluted to the desired concentration using culture medium (ensuring the diluents contained no more than 1 in 1,000 DMSO) and were prepared on-site.

Cell viability and NO inhibitory activity assays

The growth inhibition of RAW264.7 cells was evaluated using the MTT (3-(4,5-dimethylthiazol-2-yl)-2,5-diphenyltetrazolium bromide) assay. In 96-well plates, cells were seeded at a density of 6×10^3 cells/mL per well in a complete growth medium, then incubated overnight at 37 ˚C with 5% CO_2 to promote cell attachment. Subsequently, various concentrations from the lignans-enriched fraction were added to the respective wells, with untreated cells serving as the control group. Following a 24 h incubation period at 37 ˚C with 5% CO_2, 20 μL of MTT solution was added to each well, and the plates were further incubated for 4 h. Thereafter, 150 μL of DMSO solution was added to each well to dissolve the purple formazan crystals. The optical density (OD) of the formazan product was measured, reflecting a proportional measure of the number of metabolically active and surviving cells. Finally, cell viabilities after the different treatments were calculated by $(A/B) \times 100\%$, where A and B are the absorbance of treated and untreated samples, respectively.

RAW264.7 cells (1×10^4 cells/mL per well) were cultured in 96-well plates for 24 h at 37 ˚C with 5% CO_2 to allow for cell adhesion. Three groups were established: the negative control group (only containing cell culture medium), the LPS model group (containing 1 μg/mL LPS) and the drug group (1 μg/mL LPS, LPS + indomethacin, LPS + varying concentrations of the lignans-enriched fraction), with three duplicate wells included for each group. Following a 24 h incubation period at 37 ˚C with 5% CO_2, 100 μL of the supernatant was transferred to a new 96-well plate. Then, 50 μL of Griess A and 50 μL of Griess B were added to each well. The NO inhibitory activity was assessed spectrophotometrically at 546 nm in the culture supernatant.

Western blotting analysis

RAW264.7 cells were lysed using RIPA lysis buffer (S3090), supplemented with a protease inhibitor cocktail (P0013, Roche Diagnostics, Indianapolis, IN, USA). The protein concentration in the lysate was ascertained using a BCA (bicinchoninic acid) protein quantification kit (P0010S, Beyotime Biotech., Shanghai, China).

Equal amounts of protein were subjected to 10% SDS polyacrylamide gel electrophoresis (SDS-PAGE), followed by transfer onto a nitrocellulose (NC) membrane. The membrane was then blocked in TBST containing 5% non-fat dry milk. Subsequently, the membrane was incubated with a primary antibody at 4 ˚C overnight, followed by a 1 h incubation with an HRP (horseradish peroxidase)-conjugated secondary antibody. After three washes with TBST, the protein bands were visualized using a chemiluminescent gel imaging system.

Statistical analysis

Using SPSS software version 20.0, cellular experimental data were evaluated using Student’s t-test for single comparisons. Statistical significance was denoted as $^{*}P < 0.05$ and $^{**}P < 0.01$. Data were represented as the mean ± standard error of the mean.

Results

Chemical components discovery and identification

The samples of *T. jaminoides* were analyzed using UPLC-QTOF-MS, and their base peak chromatogram is presented in Figure 1. A total of forty-one components were tentatively identified, among which nine, denoted with an asterisk (*), were reported for the first time within the genus of *Trachelospermum*. These identifications were made by comparing their molecular formula and primary/secondary mass fragmentation patterns with those reported in the literature (Table 1) [1, 16–25].

Dibenzyltyrolactone-type lignans constituted the predominant portion of the biomarkers obtained, aligning with previous findings that lignans are the major bioactive constituents in *T. jaminoides* [32]. Based on the mass spectrum analysis, compounds 8 and 9 exhibited close retention times and no significant divergence in their cleavage pathways [23]. For compound 8, a peak at m/z 373.1282 was observed after the elimination of a glucose fragment (−162 Da) from the peak at m/z 535.1816. The peak at m/z 355.1205 indicates the loss of H_2O due to cleavage of the -OH in the lactone ring, where the two substituents were initially connected, followed by the loss of CO and H_2O from the lactone ring, resulting in the fragment ions of m/z 179.0706. Additionally, by comparing the retention time (t_R) with those reported, compounds 8 and 9 are tentatively identified as nortrachelogenin 5’-C-β-glucoside and nortracheloside, respectively [23]. The fragment ion m/z 387.1441 of compound 18 emerged from the adduct m/z 595.2043 $[M+HCOO]^-$ after losing one molecule of glucose fragment (−162 Da). Subsequently, a molecule of -OCH_3 was cleaved to yield the fragment ion m/z 357.1339. In conjunction with the literature and the mass spectrum fracture mode, compound 18 was assigned as tracheloside [23].

Flavonoids are readily distinguishable in *T. jaminoides*. The general cleavage behavior of flavonoid glycosides unfolds as follows: primarily, glycosides undergo a successive loss of sugar chain units,

such as rhamnose (−146 Da) or glucose (−162 Da). This sequential cleavage culminates in the formation of flavonoid aglycones. Employing an appropriate cone voltage can also induce a Retro-Diels-Alder (RDA) cleavage of the C ring in the aglycone moiety, followed by the loss of different amounts of H_2O and CO [33, 34]. The mass spectrum peak of compound 7 at m/z 447.0921 $[M-H]^-$, and its fragment ion at m/z 285.0395, which is obtained by removing one molecule of glucose fragment (−162 Da), facilitated the identification of compound 7 as luteolin 7-O-glucopyranoside [35].

Triterpenoids exhibit a propensity for substituent fracture, loss of sugar chain substituents, and RDA cleavage. The mass spectrum peak of compound 20 at m/z 727.3941 $[M+COOH]^-$, and the fragment ion m/z 519.3326 – obtained post removal of a glucose residue – led to the assignment of compound 20 as trachelosperoside B 1 [25]. The secondary mass peak at m/z 533.3104 of compound 22 is attributed to a glucose fragment fracture, followed by an adjacent fracture with carboxyl ring of cracking fragment ions leading to the peak at m/z 471.3105. Hence, compound 22 was speculated as trachelosperoside F [25].

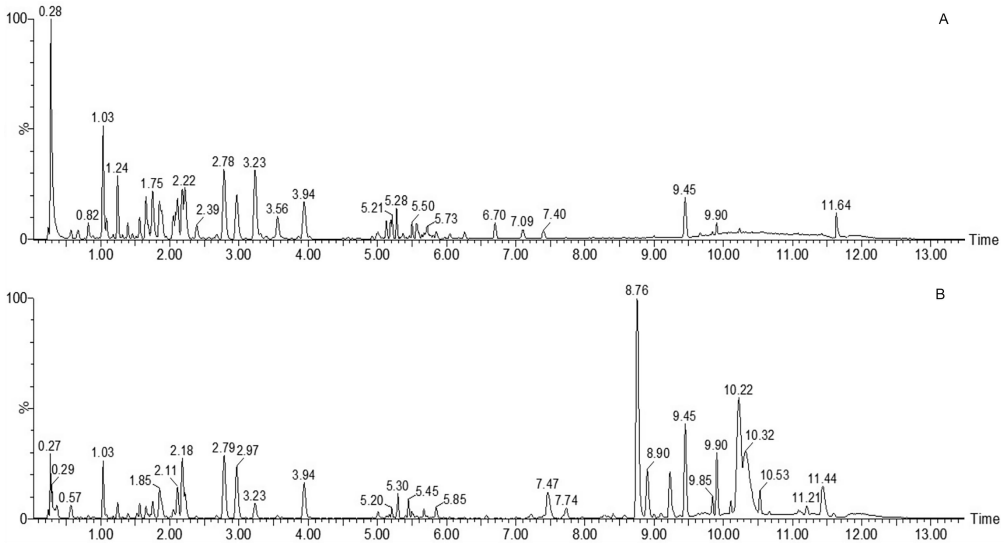

Figure 1 Base peak chromatograms of aqueous methanol extracts from *T. jaminoides*. A, Negative ion mode. B, Positive ion mode.

Table 1 Identification of chemical components from *T. jaminoides*

No.	t_R (min)	Adduct	Mass (m/z)	Main fragment ions	Molecular formula	Exact mass	Proposed compound	PubMed CID	Error (ppm)	Type
1	0.83	$[M-H]^-$	353.0867	191.0546 179.0337 161.0242 135.0441	$C_{16}H_{18}O_9$	354.0951	Caffeoylquinic acid	10155076	−0.06	Phenylpropanoids
2	1.05	$[M-H]^-$	353.0881	191.0554 179.0253 173.0357 161.0210 135.0312	$C_{16}H_{18}O_9$	354.0951	Chlorogenic acid	1794427	0.08	Phenylpropanoids
3	1.25	$[M-H]^-$	353.0877	191.0551 179.0344 173.0443 161.0238 135.0446	$C_{16}H_{18}O_9$	354.0951	Cryptochlorogenic acid	N/A	0.04	Phenylpropanoids
4	1.40	$[M-H]^-$	367.1045	191.0555 173.0439 135.0423	$C_{17}H_{20}O_9$	368.1107	Methyl chlorogenate	6476139	0.16	Phenylpropanoids
5	1.56	$[M-H]^-$	697.2361	373.1273 221.0682 191.056	$C_{32}H_{42}O_{17}$	698.2420	Nortrachelogenin 4,4'-di-O-β-D-glucopyranoside	N/A	0.19	Lignans
6	1.66	$[M-H]^-$	463.0891	301.0329 271.0240	$C_{21}H_{20}O_{12}$	464.0955	Hyperoside	5281643	0.14	Flavonoids
7	1.76	$[M-H]^-$	447.0921	285.0395 284.0317	$C_{21}H_{20}O_{11}$	448.1006	Luteolin 7-O-glucopyranoside	5280637	−0.07	Flavonoids
8	1.85	$[M-H]^-$	535.1823	373.1282 355.1205	$C_{26}H_{32}O_{12}$	536.1894	Nortrachelogenin 5'-C-β-glucoside	N/A	0.07	Lignans

Table 1 Identification of chemical components from *T. jaminoides* (*Continued*)

No.	t_R (min)	Adduct	Mass (m/z)	Main fragment ions	Molecular formula	Exact mass	Proposed compound	PubMed CID	Error (ppm)	Type
9	1.88	[M + HCOO]$^-$	581.1865	179.0706 373.1282 355.1205 179.0706	$C_{26}H_{32}O_{12}$	536.1894	Nortracheloside	45482323	−0.06	Lignans
10	2.05	[M − H]$^-$	577.1573	269.0448 150.9996	$C_{27}H_{30}O_{14}$	578.1636	Rhoifolin	5282150	0.15	Flavonoids
11	2.08	[M − H]$^-$	447.0946	300.0258 151.0021	$C_{21}H_{20}O_{11}$	448.1006	Quercetin 3-O-rhamnoside	5280459	0.18	Flavonoids
12	2.18	[M − H]$^-$	711.2511	387.1431 129.0912	$C_{33}H_{44}O_{17}$	712.2578	Trachelogenin 4'-O-β-gentiobioside	N/A	0.11	Lignans
13	2.22	[M − H]$^-$	577.1575	431.0917 269.0442 151.0025	$C_{27}H_{30}O_{14}$	578.1639	Isorhoifolin	9851181	0.14	Flavonoids
14	2.23	[M − H]$^-$	579.1721	271.0605 269.0447 151.0031	$C_{27}H_{32}O_{14}$	580.1792	Naringin	442428	0.07	Flavonoids
15	2.24	[M − H]$^-$	431.0975	269.0433 268.0369 151.0014	$C_{21}H_{20}O_{10}$	432.1056	Apigenin 7-glucoside	5280704	−0.03	Flavonoids
16	2.39	[M − H]$^-$	515.1180	353.0873 191.0549 179.0339 173.0449 135.0452	$C_{25}H_{24}O_{12}$	516.1268	4,5-Dicaffeoylquinic acid	6474309	−0.10	Phenylpropanoids
17	2.67	[M − H]$^-$	549.1987	387.1465 357.1351	$C_{27}H_{34}O_{12}$	550.2050	4-Demethyltraxillaside	168013457	0.15	Lignans
18	2.79	[M + HCOO]$^-$	595.2043	387.1441 357.1339	$C_{27}H_{34}O_{12}$	550.2050	Tracheloside	169511	0.16	Lignans
19	2.97	[M + HCOO]$^-$	741.2613	371.1499 323.0976	$C_{33}H_{44}O_{16}$	696.2629	Arctigenin 4'-β-gentiobioside	5319807	0.07	Lignans
20	3.23	[M + HCOO]$^-$	727.3941	681.3863 519.3326	$C_{36}H_{58}O_{12}$	682.3930	Trachelosperoside B1	146116086	0.34	Triterpenoids
21	3.39	[M − H]$^-$	373.1281	327.1237 179.0706	$C_{20}H_{22}O_7$	374.1366	Nortrachelogenin	394846	−0.07	Lignans
22	3.56	[M − H]$^-$	695.3642	533.3104 471.3105	$C_{36}H_{56}O_{13}$	696.3721	Trachelosperoside F	N/A	-0.01	Triterpenoids
23	3.86	[M − H]$^-$	679.3694	517.3170 455.3162	$C_{36}H_{56}O_{12}$	680.3772	Trachelosperoside A1	21637743	0.00	Triterpenoids
24	3.94	[M + HCOO]$^-$	579.2084	373.1294 371.1487	$C_{28}H_{36}O_{13}$	534.2101	Arctiin	100528	0.06	Lignans
25	4.02	[M + HCOO]$^-$	609.2185	401.1603 181.0864	$C_{28}H_{36}O_{12}$	564.2207	Traxillaside	10030789	0.01	Lignans
26	5.01	[M − H]$^-$	387.1440	357.1332 193.0865	$C_{21}H_{24}O_7$	388.1522	Trachelogenin	452855	−0.04	Lignans
27*	5.13	[M − H]$^-$	327.2169	229.1441 171.1016	$C_{18}H_{32}O_5$	328.2250	9S,12R,13S-Trihydroxy-10E,15Z-octadecadienoic acid	9949348	−0.03	Others
28	5.19	[M − H]$^-$	329.2327	229.1438 211.1323 171.1021	$C_{18}H_{34}O_5$	330.2406	9,12,13-Trihydroxy-10-octadecenoic acid	5282966	−0.01	Others
29	5.21	[M − H]$^-$	327.2166	211.1337 171.1017	$C_{18}H_{32}O_5$	328.2250	9S,12S,13S-Trihydroxy-10E,15Z-octadecadienoic acid	10936354	−0.06	Others
30	5.28	[M − H]$^-$	329.2327	201.1129 171.1024	$C_{18}H_{34}O_5$	330.2406	9,10,13-Trihydroxy-11E-octadecenoic acid	5282965	−0.01	Others
31*	5.38	[M − H]$^-$	487.3426	471.3110	$C_{30}H_{48}O_5$	488.3502	Euscaphic acid	471426	0.02	Triterpenoids

Table 1 Identification of chemical components from *T. jaminoides* (*Continued*)

No.	t_R (min)	Adduct	Mass (m/z)	Main fragment ions	Molecular formula	Exact mass	Proposed compound	PubMed CID	Error (ppm)	Type
32	5.46	$[M-H]^-$	721.3632	453.2993 487.3437 397.1352	$C_{39}H_{62}O_{12}$	722.4241	23,24-O-isopropylidene-2α,3β,19α-trihydroxyurs-12-en-28-O-β-D-glucopyranoside	N/A	−5.31	Triterpenoids
33	5.50	$[M-H]^-$	721.3645	415.1439 397.1342	$C_{39}H_{62}O_{12}$	722.4241	23,24-O-isopropylidene-2α,3α,19α-trihydroxyurs-12-en-28-O-β-D-glucopyranoside	N/A	−5.18	Triterpenoids
34*	5.56	$[M-H]^-$	293.2113	275.1997 183.0128 171.1019	$C_{18}H_{30}O_3$	294.2195	Hydroxylinolenic acid	5312775	−0.04	Others
35*	5.73	$[M-H]^-$	295.2275	279.2302 277.2163 171.1014	$C_{19}H_{36}O_2$	296.2715	Methyl oleate	5364509	−3.62	Others
36	5.80	$[M+HCOO]^-$	699.3806	653.3752 471.3438	$C_{35}H_{58}O_{11}$	654.3979	Teikaside AL Ic	N/A	−1.50	Triterpenoids
37*	5.85	$[M-H]^-$	540.3298	480.3089 452.2829	$C_{32}H_{47}NO_6$	541.3403	Aconitan-15-ol,20-ethyl-1,6,16-trimethoxy-4-(methoxymethyl)-14-(phenylmethoxy)-,(1,6,14,15,16)-(9CI)		−0.27	Alkaloids
38*	6.05	$[2M-H]^-$	571.2871	277.2176 197.9631	$C_{20}H_{18}N_2$	286.1470	Diphenylmethanone-2-(4-methylphenyl)hydrazone	N/A	0.09	Alkaloids
39*	6.18	$[M-H]^-$	311.1668	297.2414 255.2343	$C_{13}H_{28}O_8$	312.1784	6,6-Bis(2-methoxyethoxy)-2,5,7,10-tetraoxaundecane	N/A	−0.38	Others
40*	7.10	$[M-H]^-$	339.2326	279.2400 163.1118	$C_{23}H_{32}O_2$	340.2402	2,2'-Bis(4-methyl-6-tert-butylphenol) methane	8398	0.02	Others
41*	7.40	$[M-H]^-$	279.2319	199.8464 115.9211	$C_{18}H_{32}O_2$	280.2402	(Z,Z)-9,12-Octadecadienoic acid	5280450	−0.05	Others

*The first reported components in the genus *Trachelospermum L.*

Molecular docking results with iNOS protein

Lignans, flavonoids, and triterpenoids are identified as the principal active constituents of *T. jasminoides*, and their distinctive characteristics are readily delineated by this UPLC-QTOF-MS experiment [4]. Given the pivotal role of iNOS in inflammatory responses, a molecular docking study was conducted to scrutinize the interaction between these profiled compounds with the iNOS enzyme [10]. As outlined in Table 2, the docking scores are ranked from strong to weak based on the binding affinity.

Docking calculation revealed that nortrachelogenin 4,4'-di-O-β-D-glucopyranoside, trachelogenin 4'-O-β-gentiobioside, arctigenin 4'-β-gentiobioside and rhoifolin scored relatively high compared to the reference ligand, as detailed in Table 2. Specifically, the complex formed between nortrachelogenin 4,4'-di-O-β-D-glucopyranoside and iNOS (PDB ID: 3E7G) exhibited an energy of approximately −11.481 kcal/mol. The observed interactions include six hydrogen donor bonds with residues Met 120, Glu 377, and Pro 350, contributing energies of −3.5 kcal/mol, −1.7 kcal/mol, and −1.90 kcal/mol at distances of 3.53 Å, 3.00 Å, and 2.67 Å, respectively. Additionally, two hydrogen acceptor bonds to residues Arg 381 and Gly 371 had energies of −3.5 kcal/mol and −1.4 kcal/mol, at distances of 2.99 Å and 2.84 Å. There were also two arene-H interactions with residues Ile 201 and Trp 463, with energies of −0.7 kcal/mol and −0.8 kcal/mol and distances of 4.22 Å and 3.62 Å, respectively.

In contrast, the complex formed between indomethacin and iNOS exhibited an energy of −6.966 kcal/mol. This interaction was characterized by two hydrogen donor bonds to residues Glu 377 and Met 434, with energies of −2.9 kcal/mol and −0.5 kcal/mol, at distances of 2.85 Å and 3.43 Å, respectively. Additionally, an arene-arene interaction with residue Trp 194 was observed, contributing 0 kcal/mol in energy, at a distance of 3.43 Å, as illustrated in Figure 2.

Further inspection of the binding models revealed the intricate interactions between 3E7G and the other compounds. The empirical data suggested that, on a comparative scale, lignans manifest a stronger binding affinity with iNOS relative to flavonoids and triterpenoids (Supplement Figure S1–S4). Following these findings, the lignans-enriched fraction derived from *T. jasminoide* through macroporous resin extraction was employed to ascertain the NO inhibitory effect and binding affinity of iNOS protein in vitro.

Cell viability and NO inhibitory activity

As illustrated in Figure 3, cell viabilities higher than 85% were observed after LPS-induced RAW264.7 cells were exposed to the lignans-enriched fraction at the concentration less than or equal to 80 μg/mL with a dose-dependent manner. Anti-inflammatory bioassay showed the fraction demonstrated significant inhibitory effects on NO production in LPS-induced RAW264.7 cells, at the concentration of 20 μg/mL, 40 μg/mL and 80 μg/mL (Figure 4).

Inhibitory effect of the lignans-enriched fraction on iNOS protein expression

As illustrated in Figure 5, a notable augmentation in the relative protein expression of iNOS was observed in the model control group compared to the blank control group ($^{\#\#}P < 0.01$), indicating that the cell inflammation model was established after LPS addition. Relative to the model control group, a significant diminution in the relative

protein expression of iNOS in RAW264.7 cells was evident with the escalating concentration of the lignans-enriched fraction ($^{**}P < 0.01$).

Discussion

Within the *Chinese Pharmacopoeia*, the stems and leaves are designated as medicinal parts of *T. jasminoides*. Utilizing UPLC-QTOF-MS technology, it was discerned that the lignans, flavonoids, and triterpenoids constitute the primary constituents in this ethnic herbal remedy. Through molecular docking methodology, lignans in *T. jasminoides* were substantiated to possess a more robust binding affinity with iNOS, providing preliminary confirmation that lignans are the principal anti-inflammatory active components. When comparing indomethacin with nortrachelogenin 4,4'-di-O-β-D-glucopyranoside, the latter demonstrated a relatively stronger binding affinity towards the iNOS enzyme. This increased affinity may be attributed to the difference in hydrogen bonding capabilities. Indomethacin has only four hydrogen bond acceptors and two donors, whereas nortrachelogenin 4,4'-di-*O*-β-D-glucopyranoside is capable of forming sixteen hydrogen bond acceptors and nine donors. However, it is important to note that an excessive number of hydrogen bond donors and acceptors can diminish the druggability of nortrachelogenin 4,4'-di-*O*-β-D-glucopyranoside [36].

Table 2 Glide score and binding interaction of major active compounds in *T. jasminoides* with human iNOS

Compounds	Docking score (kcal/mol)	Interactions
Nortrachelogenin 4,4'-di-O-β-D-glucopyranoside	−11.481	Met 120, Ile 201, Pro 350, Gly 371, Glu 377, Arg 381, Trp 463
Trachelogenin 4'-O-β-gentiobioside	−11.026	Trp 194, Glu 377, Arg 381, Trp 463
Arctigenin 4'-β-gentiobioside	−10.780	Trp 194, Glu 377, Arg 381, Trp 463
Rhoifolin	−10.117	Arg 199, Met 355, Glu 377, Met 434
Traxillaside	−9.665	Cys 200, Trp 372, Met 434
Tracheloside	−9.544	Ile 201, Gly 202, Trp 372, Tyr 489
4-Demethyltraxillaside	−9.540	Arg 199, Cys 200, Trp 372, Met 434
Arctiin	−9.381	Trp 372, Phe 476
Isorhoifolin	−9.229	Met 120, Trp 194, Arg 381, Trp 463
Nortrachelogenin 5'-C-β-glucoside	−9.172	Met 120, Trp 372, Glu 377, Met 434, Trp 463
Naringin	−9.125	Gly 202, Phe 369, Trp 372, Glu 377, Trp 463
Nortracheloside	−9.024	Met 120, Gly 202, Gly 371, Arg 381, Met 434
Apigenin 7-glucoside	−8.991	Trp 194, Gly 202, Met 355, Trp 372, Tyr 491
Luteolin 7-O-glucopyranoside	−8.358	Cys 200, Ile 201, Trp 372, Glu 377
Hyperoside	−8.145	Trp 194, Cys 200, Trp 372, Glu 377
Quercetin 3-O-rhamnoside	−8.013	Arg 381, Asp 385, Arg 388, Trp 463
Trachelogenin	−7.470	Cys 200, Gly 202, Glu 377
Nortrachelogenin	−7.283	Cys 200, Trp 372, Trp 463
Euscaphic acid	−7.174	Cys 200, Lle 201, Met 355, Trp 372
Indomethacin*	−6.966	Trp 194, Glu 377, Met 434

*Standard inhibitor.

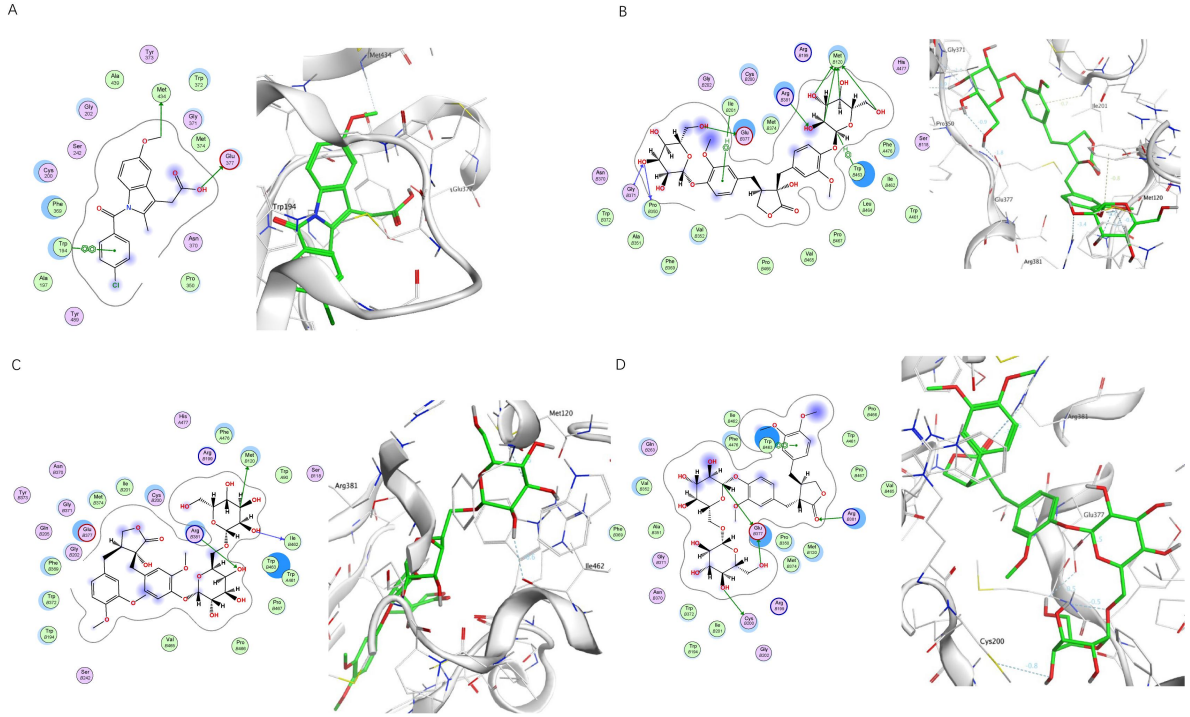

Figure 2 Molecular interactions between top 3 active compounds in *T. jasminoides* with human iNOS. A, Indomethacin. B, Nortrachelogenin 4,4'-di-O-β-D-glucopyranoside. C, Trachelogenin 4'-O-β-gentiobioside. D, Arctigenin 4'-β-gentiobioside.

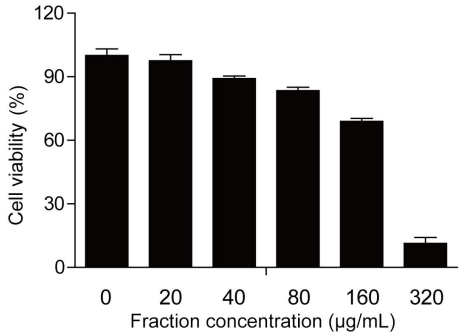

Figure 3 Effects of the lignans-enriched fraction in *T. jasminoides* on the viability of RAW264.7 cells ($\bar{x} \pm s$, n = 3)

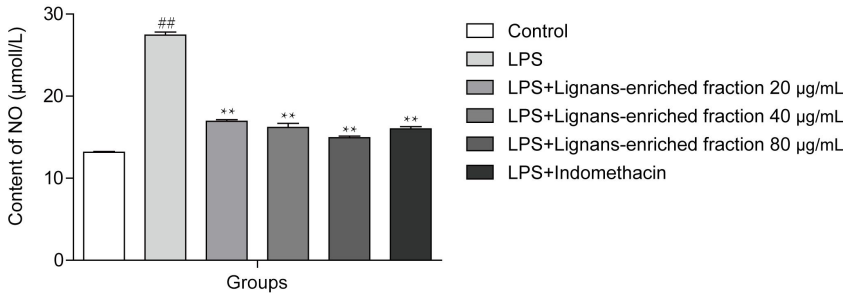

Figure 4 Inhibitory effects of the lignans-enriched fraction on NO production in LPS-induced RAW264.7 cells ($\bar{x} \pm s$, n = 3)

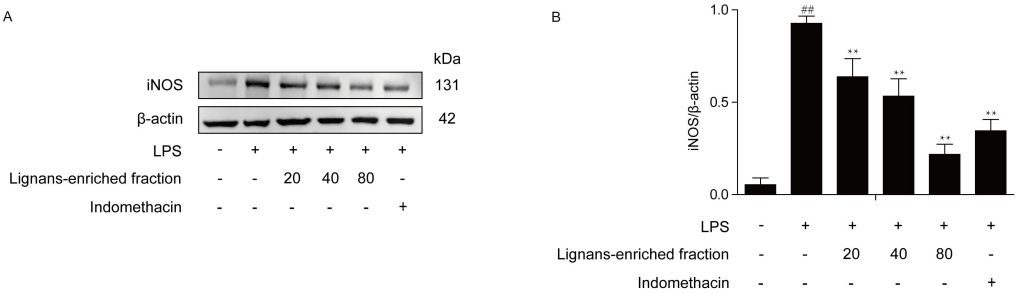

Figure 5 Effects of the lignans-enriched fraction for 24 h on the expression of iNOS. A, Representative image of iNOS protein expression in cells treated with the lignans-enriched fraction from *T. jasminoides*. B, Statistical data analysis, $\bar{x} \pm s$, n = 3. Compared with the blank control, $^{\#\#}P < 0.01$, compared with the model control, $^{**}P < 0.01$.

Our antecedent study illustrated that most lignans from *T. jaminoides* curtailed the production of NO, thereby manifesting anti-inflammatory activity [16]. Lignans have been demonstrated to mitigate inflammatory reactions by stifling the production or expression of inflammatory mediators [37]. Certain specific lignans, for instance, arctigenin has been reported to diminish the expression of iNOS and further reduce the aggregate production of NO by inhibiting the nuclear transmigration of transcription factor p65, thus playing an anti-inflammatory role [38]. Trachelogenin, nortrachelogenin, and tracheloside have been revealed to inhibit the production of tumor necrosis factor-alpha and interleukin-1 beta through in vivo experiments [39]. Trachelogenin and arctigenin have been found to exhibit anti-inflammatory activities on the IFN-γ/STAT1 pathway. Moreover, trachelogenin, arctigenin, and matairesinol have been ascertained to strongly inhibit the IL-6/STAT3 pathway. These compounds have the potential to modulate this pathway and may consequently alleviate inflammation [40].

In the present study, lignans from *T. jasminoides* identified through UPLC-QTOF-MS demonstrated notable interactions with the iNOS enzyme during molecular docking analysis. The lignan-enriched fraction was further confirmed to substantially inhibit NO release and reduce iNOS protein expression in vitro. To validate the therapeutic efficacy of this medicinal plant and elucidate its mechanism of action, in vivo experiments are planned for the near future.

Conclusion

In conclusion, this investigation posits lignans as the plausible bioactive constituents of *T. jasminoides,* corroborated by experimental data and literature retrieve. In addition, nine constituents, reported for the first time within this genus, are presented herein, thereby enriching the chemical diversity of *T. jasminoides*. Importantly, this study underscores that the lignans-enriched fraction from *T. jasminoides* exhibits discernible NO inhibitory activity, holding significant promise to advance the rational utilization of ethnic herbal medicine resources.

References

1. Zhao Z, He X, Zhao Y, et al. Phytochemistry, pharmacology and traditional uses of plants from the genus Trachelospermum L. *Molecules* 2017;22(9):1406. Available at: http://doi.org/10.3390/molecules22091406
2. Wang J. Research status of ethnic medicine in the treatment of gouty arthritis. *Lishizhen Med Mater Med Res* 2014;25(8):1958–1960. (Chinese) Available at: https://kns.cnki.net/kcms2/article/abstract?v=ZJxhFRRmSIg6-3MMsCF_7BkB1PRTS_nppWTJBG2sXl2EGF2S3r0z0j8xr8VsIdYk_SkRmS5dpL30jPSw3bEPiP6mdjCkVsONlgcXunu61F_xcS55_eGy1Q==&uniplatform=NZKPT
3. Jiang T, Kong B, Yan W, et al. Network pharmacology to identify the pharmacological mechanisms of a traditional

Chinese medicine derived from Trachelospermum jasminoides in patients with rheumatoid arthritis. *Med Sci Monit* 2020;26:e992639. Available at: http://doi.org/10.12659/MSM.922639
4. Li JS, Zhang Q, Zhang T, et al. Research progress of traditional Chinese medicine of Trachelospermum jasminoides. *J Hebei TCM Pharmacol* 2016;31(2):55–58. (Chinese) Available at: http://doi.org/10.16370/j.cnki.13-1214/r.2016.02.020
5. Hankittichai P, Buacheen P, Pitchakarn P, et al. Artocarpus lakoocha extract inhibits LPS-induced inflammatory response in RAW 264.7 macrophage cells. *Int J Mol Sci* 2020;21(4):1355. Available at: http://doi.org/10.3390/ijms21041355
6. McGettrick AF, O'Neill LAJ. How metabolism generates signals during innate immunity and inflammation. *J Biol Chem* 2013;288(32):22893–22898. Available at: http://doi.org/10.1074/jbc.R113.486464
7. An J, Ryu G, Shin SA, et al. Wistin exerts an anti-inflammatory effect via nuclear factor-κB and p38 signaling pathways in lipopolysaccharide-stimulated RAW264.7 cells. *Molecules* 2022;27(17):5719. Available at: http://doi.org/10.3390/molecules27175719
8. Subedi L, Gaire BP, Kim SY, Parveen A. Nitric Oxide as a target for phytochemicals in anti-neuroinflammatory prevention therapy. *Int J Mol Sci* 2021;22(9):4771. Available at: http://doi.org/10.3390/ijms22094771
9. Ferreira SS, Martins-Gomes C, Nunes FM, et al. Elderberry (Sambucus nigra L.) extracts promote anti-inflammatory and cellular antioxidant activity. *Food Chem X* 2022;15:100437. Available at: http://doi.org/10.1016/j.fochx.2022.100437
10. Kang J, Zhang Y, Cao X, et al. Lycorine inhibits lipopolysaccharide-induced iNOS and COX-2 up-regulation in RAW264.7 cells through suppressing P38 and STATs activation and increases the survival rate of mice after LPS challenge. *Int Immunopharmacol* 2012;12(1):249–256. Available at: http://doi.org/10.1016/j.intimp.2011.11.018
11. Chen GL, Fan MX, Wu JL, et al. Antioxidant and anti-inflammatory properties of flavonoids from lotus plumule. *Food Chem* 2019;277:706–712. Available at: http://doi.org/10.1016/j.foodchem.2018.11.040
12. Potterat O. Goji (Lycium barbarum and L. chinense): Phytochemistry, pharmacology and safety in the perspective of traditional uses and recent popularity. *Planta Med* 2009;76(1):7–19. Available at: http://doi.org/10.1055/s-0029-1186218
13. Balkrishna A, Verma S, Tiwari D, Srivastava J, Varshney A. UPLC-QToF-MS based fingerprinting of polyphenolic metabolites in the bark extract of Boehmeria rugulosa Wedd. *J Mass Spectrom* 2022;57(11):e4890. Available at: http://doi.org/10.1002/jms.4890
14. Garran TA, Ji R, Chen JL, et al. Elucidation of metabolite isomers of Leonurus japonicus and Leonurus cardiaca using discriminating metabolite isomerism strategy based on ultra-high performance liquid chromatography tandem quadrupole time-of-flight mass spectrometry. *J Chromatogr A* 2019;1598:141–153. Available at: http://doi.org/10.1016/j.chroma.2019.03.059
15. Chen L, Yu J. Modulation of Toll-like receptor signaling in innate immunity by natural products. *Int Immunopharmacol* 2016;37:65–70. Available at: http://doi.org/10.1016/j.intimp.2016.02.005
16. Song H, Tan J, Ma R, et al. Anti-inflammatory constituents from Caulis Trachelospermi. *Planta Med* 2021;88(09–10):721–728. Available at: http://doi.org/10.1055/a-1712-8209
17. Tan XQ, Guo LJ, Qiu YH, et al. Chemical constituents of Trachelospermum jasminoides. *Nat Prod Res* 2010;24(13):1248–1252. Available at: http://doi.org/10.1080/14786410903244962
18. Jing L, Yu NJ, Zhao YM, et al. Trace chemical constituents contained in Trachelospermum jasminoides and structure identification. *China J Chin Mat Med* 2012;37(11):1581–1585. (Chinese) Available at: https://kns.cnki.net/kcms2/article/abstract?v=tc18asgQl7Q_4jOiPR2uyNiLCpWR35bbnVZlg1BM3GhIUziTESkyvj-iOYca_vhDjHwZAnfLiSI1-tLlHgZ3jO-SkXPhCN8g394jrZIjQ7X4SG_7dhic7eLQph7mypzSbS4SHO7FExM=&uniplatform=NZKPT&language=CHS
19. Lee J, Yang HS, Jeong H, et al. Targeted isolation of lignans from Trachelospermum asiaticum using molecular networking and hierarchical clustering analysis. *Biomolecules* 2020;10(3):378. Available at: https://doi.org/10.3390/biom10030378
20. Zhang J, Yin ZQ, Liang JY. A new isoflavonoid glycoside from the aerial parts of Trachelospermum jasminoides. *Chin J Nat Med* 2013;11(3):274–276. Available at: http://doi.org/10.1016/S1875-5364(13)60028-X
21. Tan XQ, Chen HS, Liu RH, et al. Lignans from Trachelospermum jasminoides. *Planta Med* 2005;71(1):93–95. Available at: http://doi.org/10.1055/s-2005-837761
22. Nishibe S, Hisada S, Inagaki I. Lignans of Trachelospermum asiaticum var. intermedium. VII. Chemical proof of the position of D-glucose linkage in tracheloside and discussion of trachelogenin derivatives. *Yakugaku Zasshi* 1973;93(4):541–545. Available at: http://doi.org/10.1248/yakushi1947.93.4_541
23. Liu XT, Wang XG, Xu R, et al. Qualitative and quantitative analysis of lignan constituents in Caulis Trachelospermi by HPLC-QTOF-MS and HPLC-UV. *Molecules* 2015;20(5):8107–8124. Available at: http://doi.org/10.3390/molecules20058107
24. Atta-ur-Rahman, Fatima T, Nisa M, et al. Indole alkaloids from Trachelospermum jasminoides. *Planta Med* 1987;53(1):57–59. Available at: http://doi.org/10.1055/s-2006-962620
25. Tan XQ, Chen HS, Zhou M, et al. Triterpenoids from canes with leaves of Trachelospermum jasminoides. *Chin Tradit Herb Drugs* 2006;37(2):171–174. (Chinese) Available at: https://kns.cnki.net/kcms2/article/abstract?v=tc18asgQl7RAGk9c_aezxY8CXWfatcCBDhA7oK1NIglHOb3H1lY0Z2zndERQuCLh2oaBmGEU_3QJNeWXmyjqClFQVon_H9Zd3nSvBEMtohFYTIfCvHlPn7gtWksNDWgg7gWnYhwoW1o=&uniplatform=NZKPT&language=CHS
26. Garcin ED, Arvai AS, Rosenfeld RJ, et al. Anchored plasticity opens doors for selective inhibitor design in nitric oxide synthase. *Nat Chem Biol* 2008;4(11):700–707. Available at: http://doi.org/10.1038/nchembio.115
27. Kalathiya U, Padariya M, Baginski M. Structural, functional, and stability change predictions in human telomerase upon specific point mutations. *Sci Rep* 2019;9(1):8707. Available at: http://doi.org/10.1038/s41598-019-45206-y
28. Wojciechowski M, Lesyng B. Generalized born model: Analysis, refinement, and applications to proteins. *J Phys Chem B* 2004;108(47):18368–18376. Available at: http://doi.org/10.1021/jp046748b
29. Mohamed MY, Masocha W. Indomethacin augments lipopolysaccharide-induced expression of inflammatory molecules in the mouse brain. *PeerJ* 2020;8:e10391. Available at: http://doi.org/10.7717/peerj.10391
30. Liu MP, Yu NJ, Zhao J, et al. Quantitative analysis of total lignans in the lignan extract from Trachelospermum jasminoides by ultraviolet spectrophotometry. *Pharm J Chin PLA* 2010; 26(2):162–164. (Chinese) Available at: https://kns.cnki.net/kcms2/article/abstract?v=_AqZbjAWWJQsnJkN84pwDX5rOUyv2aKO80Lb6rttLeDjPB75LYSyyA4LAInhR8x6XCszG3zciVNRvI8etu89_6zgR_T3arvyDiSP2tQQz2Zg70Hho

TnQNogYzxSyhxlL&uniplatform = NZKPT&language = CHS
31. Zhu C, Jing L, Yu N, et al. A new lignan and active compounds inhibiting NF-κB signaling pathway from Caulis Trachelospermi. *Acta Pharm Sin B* 2013; 3(2):109–112. Available at: https://doi.org/10.1016/j.apsb.2013.02.004
32. Yu NJ, Liu MP, Zhao YM. Specificity of dual wavelength spectrophotometric quantitative analysis of total lignans in extract from Trachelospermum jasminoides. *J Int Pharm Res* 2011;38(6):470–474. (Chinese) Available at: https://kns.cnki.net/kcms2/article/abstract?v = tc18asgQl7TngJwqBW-ra07cuw3XdW_lE2LQikc7T2j_p9ty9LBx0Fe7kCIYeflL4uVKfrVoDnxXX_jWsbKnYz_COg_qNICBCZOaeTZgmybUKaW2qzCDephLB9a1UQzB8dZ_7JpSC3s = &uniplatform = NZKPT&language = CHS
33. Ali A, Bashmil YM, Cottrell JJ, et al. LC-MS/MS-QTOF screening and identification of phenolic compounds from Australian grown herbs and their antioxidant potential. *Antioxidants* (*Basel*) 2021;10(11):1770. Available at: http://doi.org/10.3390/antiox10111770
34. Qian Z, Li H, Li P, et al. Simultaneous quantification of seven bioactive components in Caulis Lonicerae Japonicae by high performance liquid chromatography. *Biomed Chromatogr* 2007;21(6):649–654. Available at: http://doi.org/10.1002/bmc.803
35. Xu ML, Wang YY, Yu M, et al. Study on chemical components of aqueous extraction from Callicarpa nudiflora by UPLC-Q-TOF-MS/MS. *Nat Prod Res Dev* 2022;34(1):42–49. (Chinese) Available at: http://doi.org/10.16333/j.1001-6880.2022.1.006
36. Benet LZ, Hosey CM, Ursu O, et al. BDDCS, the Rule of 5 and drugability. *Adv Drug Deliv Rev* 2016;101:89–98. Available at: http://doi.org/10.1016/j.addr.2016.05.007
37. Nakano Y, Nasu M, Kano M, et al. Lignans from guaiac resin decrease nitric oxide production in interleukin 1β-treated hepatocytes. *J Nat Med* 2016;71(1):190–197. Available at: http://doi.org/10.1007/s11418-016-1048-3
38. Cho MK, Park JW, Jang YP, et al. Potent inhibition of lipopolysaccharide-inducible nitric oxide synthase expression by dibenzylbutyrolactone lignans through inhibition of I-κBα phosphorylation and of p65 nuclear translocation in macrophages. *Int Immunopharmacol* 2002;2(1):105–116. Available at: http://doi.org/10.1016/S1567-5769(01)00153-9
39. Maha S, Seham EH, Ola M, et al. In vivo TNF- and IL-1 inhibitory activity of phenolics isolated from Trachelospermum jasminoides (Lindl.) Lem. *J Med Plants Res* 2015;9(2):30–41. Available at: http://doi.org/10.5897/JMPR2014.5705
40. Liu XT, Wang ZX, Yang Y, et al. Active components with inhibitory activities on IFN-γ/STAT1 and IL-6/STAT3 signaling pathways from Caulis Trachelospermi. *Molecules* 2014;19(8):11560–11571. Available at: http://doi.org/10.3390/molecules190811560